Supporting Information

Dual-Function Tetramethylammonium Fluoride Additive for High Utilization Aqueous Zinc-Ion Batteries

Bo Xiao[a], Canglong Li[b] ,Risheng Cheng[a], Tiancheng You[a], Qiwen Zhao[a], Yanzi Deng[a], Bingang Xu[c], Yuejiao Chen*[a], Libao Chen[a]

a State Key Laboratory of Powder Metallurgy, Central South University, Changsha, 410083, P. R. China.

b School of Minerals Processing and Bioengineering, Central South University, Changsha, 410083, P. R. China.

c Nanotechnology Center, Research Institute for Intelligent Wearable Systems, The Hong Kong Polytechnic University, Hung Hom, Kowloon, Hong Kong, 999077, China.

E-mail:cyj.strive@csu.edu.cn

Experimental Section

Electrolyte Preparation

$ZnSO_4 \cdot 7H_2O$ (AR, traditional Chinese medicine) was dissolved in DI water to prepare 2 M $ZnSO_4$ (marked as BE) electrolyte. For electrolytes with added Tetramethylammonium fluoride (AR Aladdin) (named as NF), different concentrations of TMAFl were dissolved in 2 M $ZnSO_4$ (25, 50 and 100 mM). For full cells, 2 M $Zn(CF_3SO_3)_2$ (AR Aladdin) was prepared by dissolving $Zn(CF_3SO_3)_2$ in DI water and 50 mM TMAF was dissolved in 2 M $Zn(CF_3SO_3)_2$.

Cathode Preparation

The potassium vanadate (KVO) cathode powder was fabricated by hydrothermal method. At first, 24 mM $H_2C_2O_4 \cdot 2H_2O$ was dissolved in 80 mL ultrapure water and magnetically stirred until limpid; then 8 mM V_2O_5 powder was mixed with the transparent solution and jointly stirred at normal temperature for 12 h. Next, 24 mM $K_2S_2O_8$ was added into the solution under magnetic stirring for 30 min. Afterwards, the mixture was put into 100 mL Teflon autoclaves and heated up to 180 ℃ for 3 h. Finally, the deep green powder was gathered by suction filtration, rinsed by ultrapure water and anhydrous ethanol successively, and dried at 60 ℃ for 12 h.

A certain quality of KVO material, Acetylene black, and PTFE dispersion were mixed in a ratio of 7:2:1, using anhydrous ethanol as the solvent to prepare a slurry. Then the agglomerated slurry was pressed onto a titanium mesh current collector and dried at 60 ℃ to remove residual solvents. The dried electrode was cut into circular pieces with a diameter of 12 mm to obtain KVO cathode material.

Characterizations

The surface morphologies were observed by scanning electron microscopy (SEM) (TESCAN MIRA3 LMH). The phase structure of samples was conducted by X-ray diffraction (XRD) (Rigaku D/Max-2550 VB Cu Kα radiation, λ=1.5406 Å). Raman spectroscopy was obtained by WITec alpha300R using a 532 nm diode-pumped solid-state laser between 4000 cm^{-1} and 100 cm^{-1}. Fourier transform infrared (FTIR) were gathered by Thermo Scientific Nicolet iS20 is between 4000 cm^{-1} and 400 cm^{-1}. The contact angles of electrolytes on the Zn foil were tested by using the static contact angle measurements (Chengde Dingsheng JY-82C Video Contact Angle Tester).

Electrochemical measurements

Testing-batteries were assembled by CR2032 cell case and Whatman glass fiber separators. A number of electrochemical performances tests, consisting of linear sweep voltammetry (LSV), Tafel analysis, electrochemical impedance spectroscopy (EIS) ranging from 100000 to 0.1 Hz, chronoamperometry (CA), and cyclic voltammetry (CV) were conducted, utilizing an Ivium electrochemical workstation from the Netherlands.

Computational details

The molecular electrostatic potential (ESP) surfaces and the frontier molecular orbital (HOMO-LUMO) energy levels of the additive molecule were calculated using the Gaussian 16 software package. Geometry optimization and single-point energy calculations were performed at the B3LYP/6-311+G(d,p) level of theory. The

electrostatic potential was mapped onto the electron density isosurface (0.001 e/Å^3) to visualize regions of electrophilic and nucleophilic reactivity. The HOMO and LUMO energy levels were extracted to evaluate the electron-donating and electron-accepting capabilities of the molecule, respectively. The energy convergence criterion was set to 10^{-6} Hartree for all calculations.

Supplementary Figures

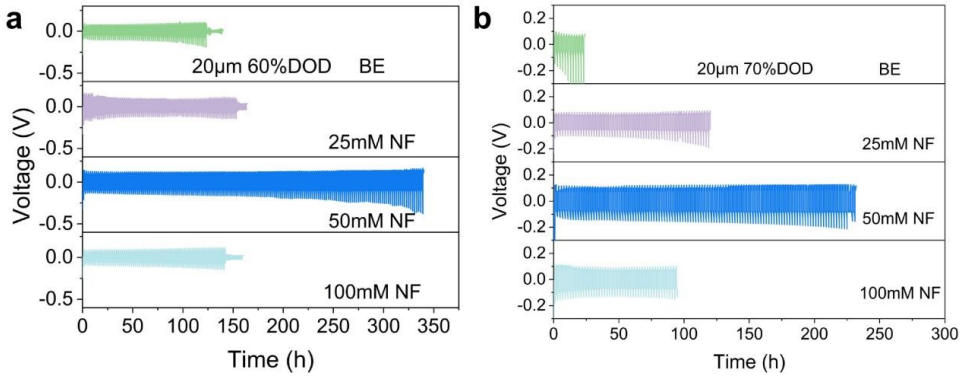

Fig.S1 The cycling performance of each concentration under the utilization conditions of a)60% and b)70%.

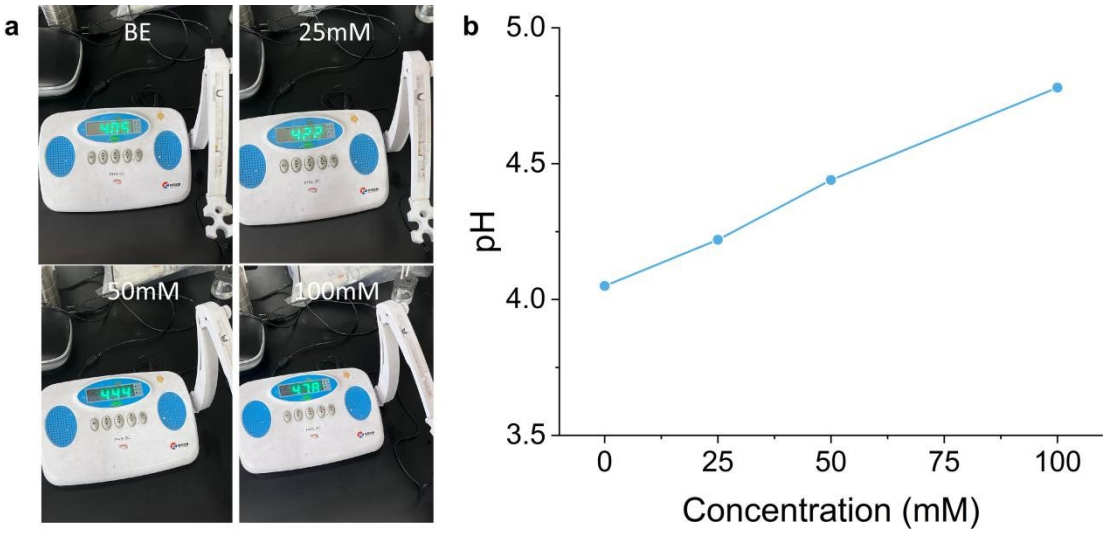

Fig.S2 a) Optical image of pH test; b) The pH values of electrolytes of different concentrations.

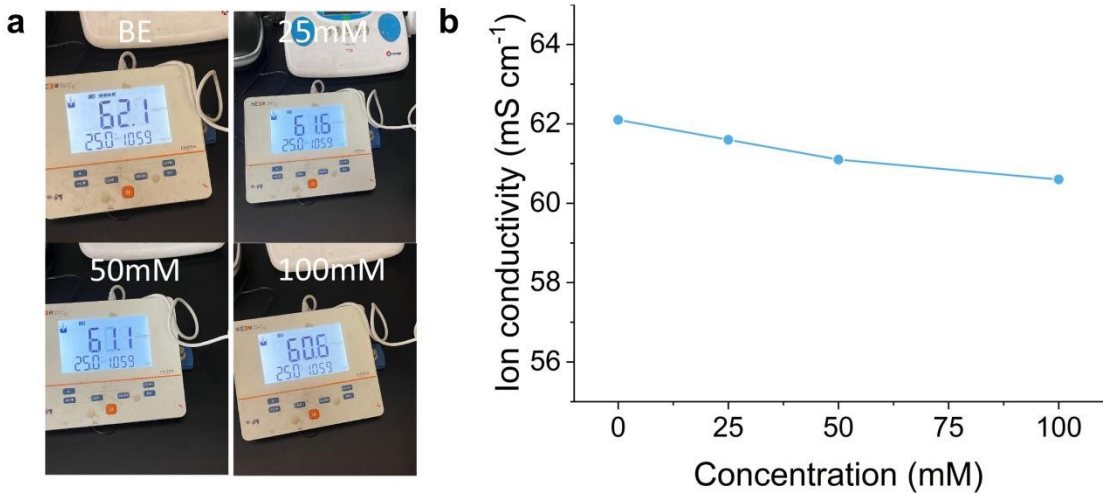

Fig.S3 a) Optical photographs of ionic conductivity tests; b) Ionic conductivity of electrolytes of different concentrations.

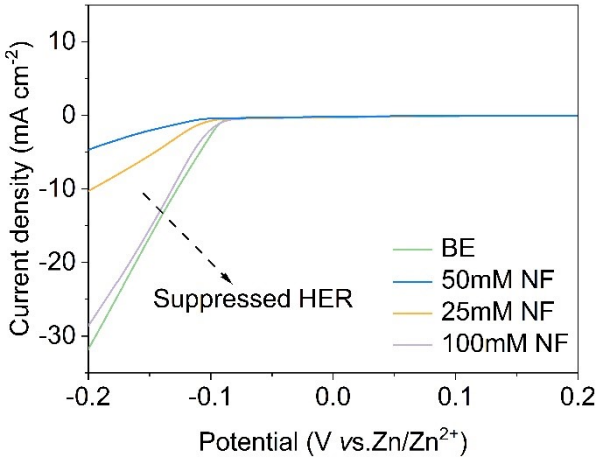

Fig.S4 The LSV curves of the Zn//Ti half-cell in different concentrations of electrolyte

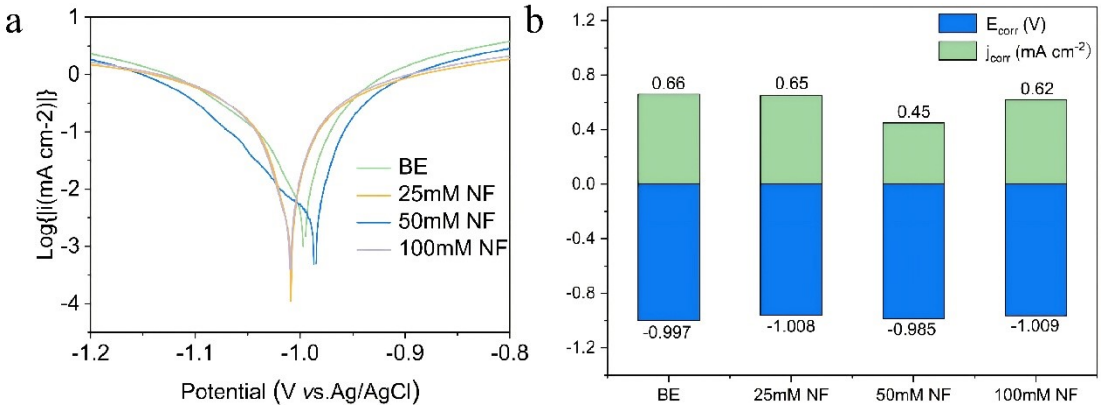

Fig.S5 a) Tafel curves of different concentrations of electrolyte in a three-electrode system; b) The obtained corrosion potential and corrosion current after fitting

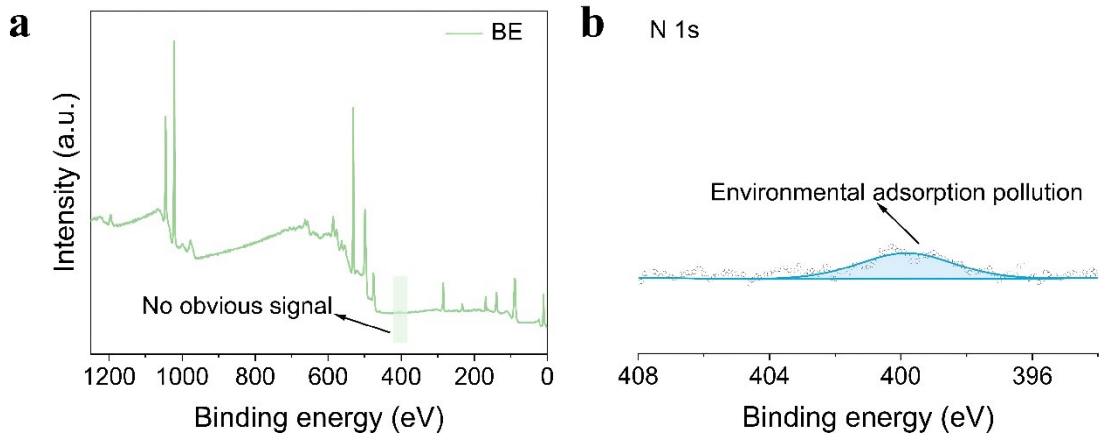

Fig.S6 XPS spectrum of Zn foil soaked in BE a) the full spectrum; b) N 1s fine spectrum.

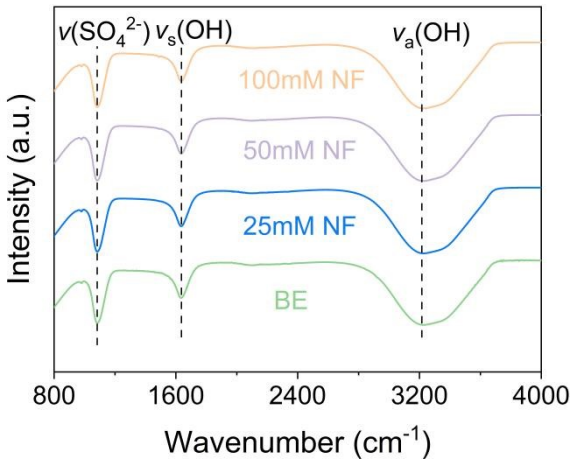

Fig.S7 Infrared full spectra of electrolytes of different concentrations.

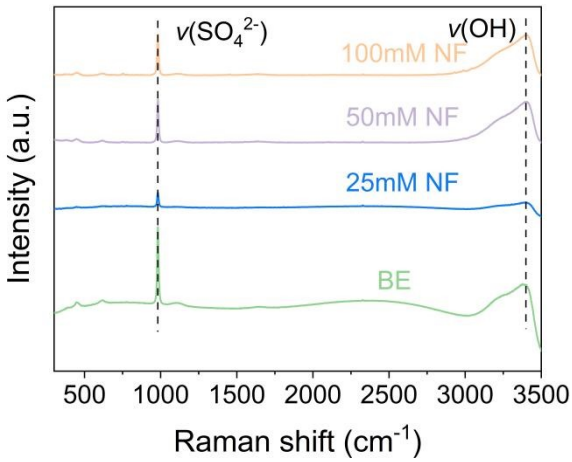

Fig.S8 Raman full spectra of electrolytes of different concentrations.

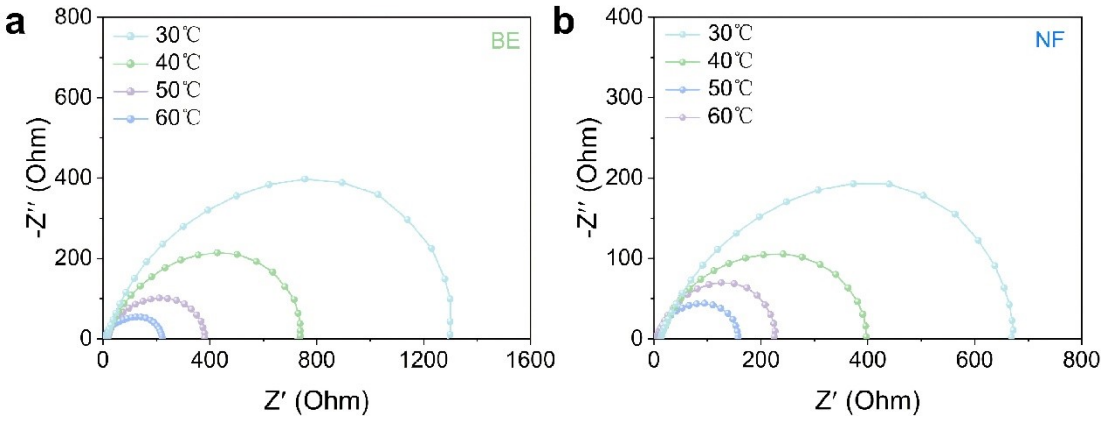

Fig.S9 a) The variable temperature impedance of the comparison group; b) The variable-temperature impedance of the experimental group.

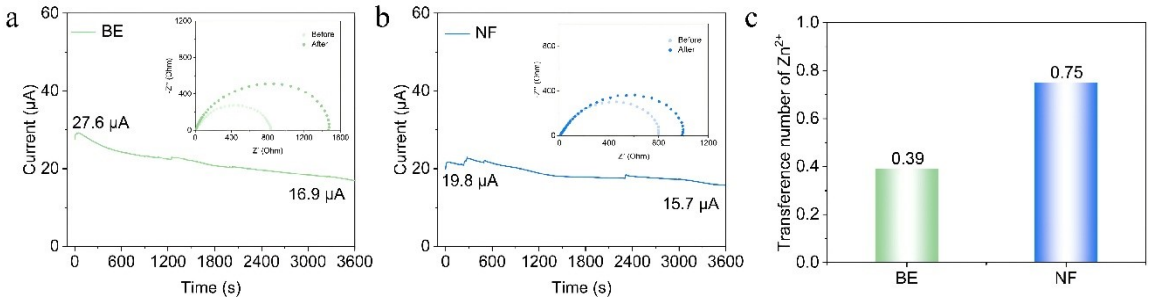

Fig.S10 Current−time plots of a) BE and b) NF symmetric cells after polarization for 3600 s at constant potential (20 mV). The insets are Nyquist plots before and after polarization; c) Transference numbers of Zn^{2+} in different electrolytes.

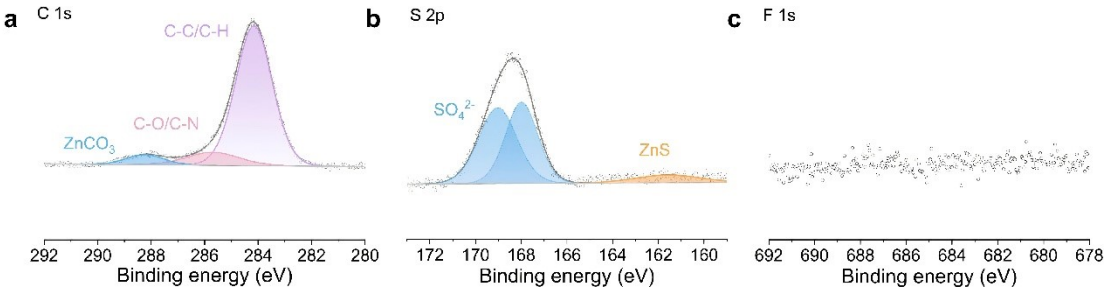

Fig.S11 a) C 1s b) S 2p c) F 1s XPS spectra of cycled Zn anode in BE

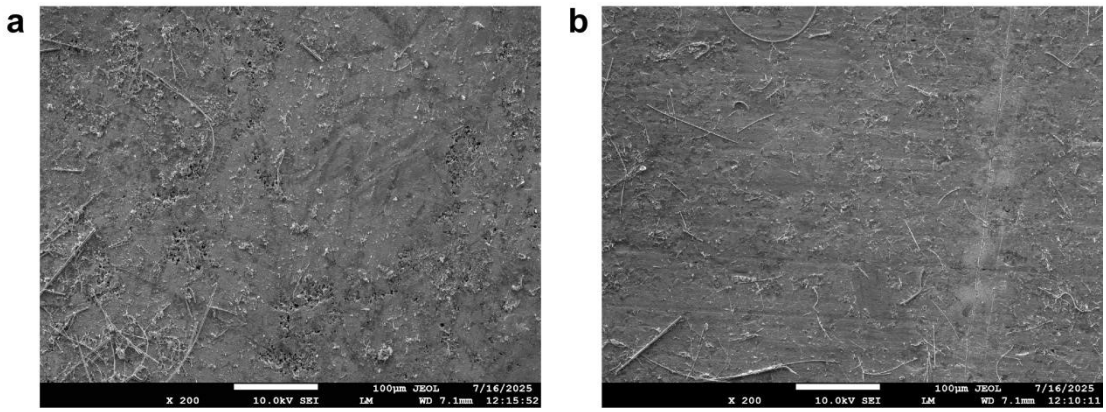

Fig.S12 A scanning electron microscope image magnified 200 times a) The surface morphology of the electrode sheet after cycling in pure $ZnSO_4$ electrolyte; b) The surface morphology of the electrode sheet after cycling in $ZnSO_4$+NF electrolyte.

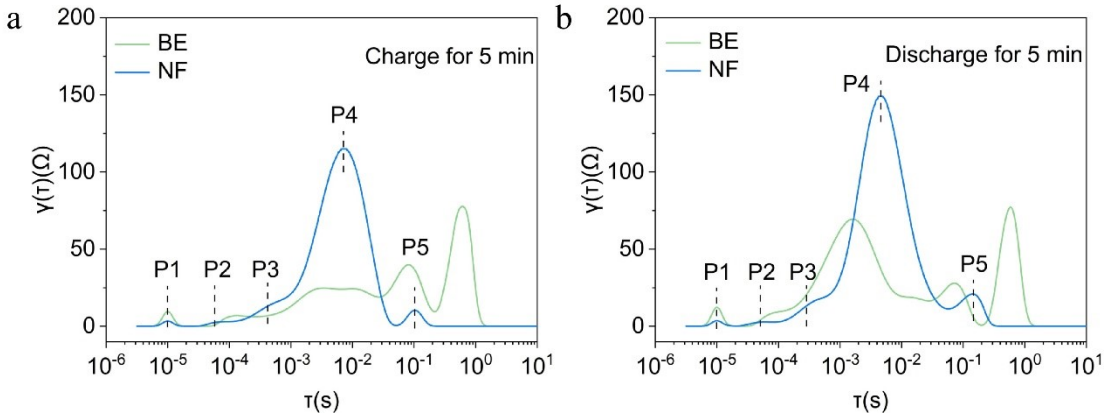

Fig.S13 DRT **plo**ts of Zn//Zn symmetric cells after a) charging and b) discharging at 1 mA cm^{-2} for 5 min

P1: relaxation of electrons at Zn metal anode.

P2: adsorption of $Zn(H_2O)_6^{2-}$.

P3: desolvation of $Zn(H_2O)_6^{2-}$.

P4: migration and crystallization of Zn ions and atoms.

P5: charge transfer across the interfaces.

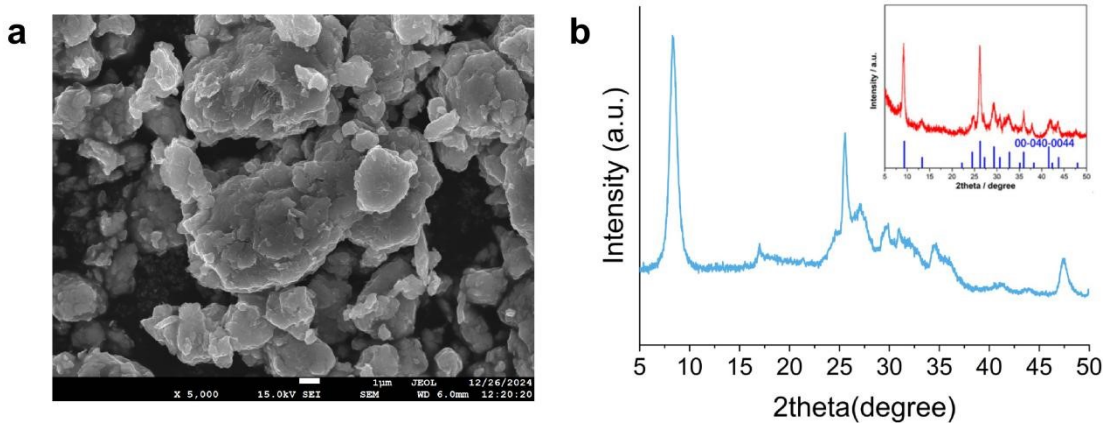

Fig.S14 a) A scanning electron microscope image of the KVO cathode magnified 5000 times; b) The XRD pattern of KVO powder.

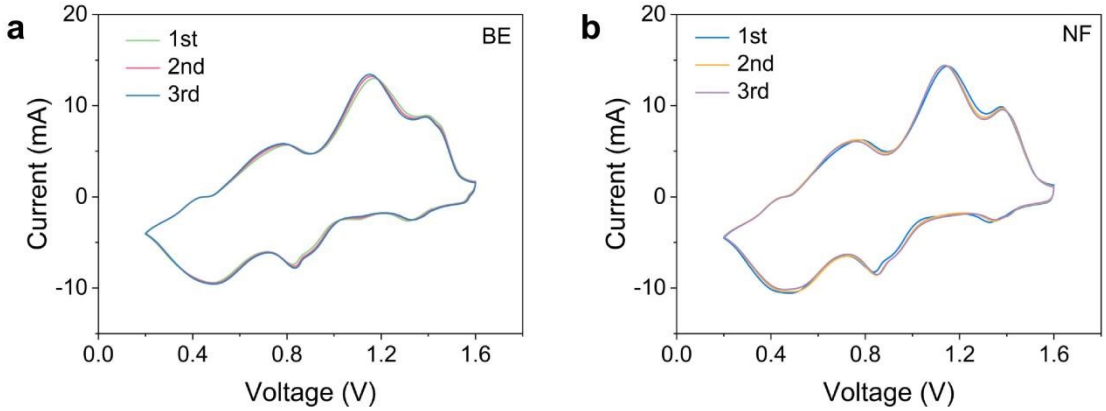

Fig.S15 a) The first three turns of the cv curve of the comparison group; b) The first three turns of the cv curve of the experimental group.